Journal of Molecular Catalysis A: Chemical 387 (2014) 92–102

Contents lists available at ScienceDirect

Journal of Molecular Catalysis A: Chemical

journal homepage: www.elsevier.com/locate/molcata

Insight into the role of fluorinated dendrimers in ruthenium(II) catalyst for asymmetric transfer hydrogenation: The stabilizing effects from experimental and DFT approach

Wei-Wei Wang[a,*], Zhi-Ming Li[b,*], Ling Su[b], Quan-Rui Wang[b], Ying-Li Wu[a]

[a] Department of Pathophysiology, Shanghai Universities E-Institute for Chemical Biology, Key Laboratory of Cell Differentiation and Apoptosis of the Chinese Ministry of Education, Shanghai Jiao Tong University School of Medicine, 227 South Chongqing Road, Shanghai 200025, PR China
[b] Department of Chemistry, Fudan University, 220 Handan Road, Shanghai 200433, PR China

ARTICLE INFO

Article history:
Received 17 December 2013
Received in revised form 20 February 2014
Accepted 25 February 2014
Available online 5 March 2014

Keywords:
Asymmetric transfer hydrogenation
Supported catalysis
Fluorinated dendrimer
Density functional calculations

ABSTRACT

A series of fluorinated dendritic chiral ligands have been designed and synthesized. These fluorinated dendrimers are capable of forming a well-defined semi-rigid structure, which was revealed to play a vital role in the ruthenium(II) bifunctional catalyst for asymmetric transfer hydrogenation of prochiral ketone substrates. In contrast to the classical non-fluorinated dendrimer carrier, both NMR and DFT study exhibit that the introduction of fluorine atoms leads to considerable intramolecular weak interactions such as π–π stacking and hydrogen bonding interactions, which make the dendritic backbone exist with a semi-rigid structure in the catalyst. This influences the performance of the catalytic center in terms of the stability and reusability. This concept was employed as a strategy to design a new Ru(II)-complex catalyst Ru-G-2′-F, which demonstrated obviously improved recycling ability up to fifteen times. Significantly enhanced activity, high enantioselectivity and outstanding recycling ability have also been achieved even at high reaction temperature with Ru-G-2-F.

1. Introduction

Asymmetric transfer hydrogenation (ATH) reactions catalyzed by chiral transition-metal complexes provide a fundamental tool for the preparation of optically active organic compounds [1]. Since the pioneer work by Noyori, Ikariya and Hashiguchi reported in the mid-1990s [2], the phosphine-free Ru catalysts bearing *N*-sulfonated 1,2-diamines as chiral ligands, which coupled with 2-propanol [2a] or HCO_2H-NEt_3 azeotropic mixture [2b] and HCO_2Na [3] as hydrogen source, have evolved to a class of effective catalysts for asymmetric transfer hydrogenation of prochiral ketones. Noyori first proposed that both an amidoruthenium complex with a square-planer geometry and a coordinatively saturated hydrido(amine)ruthenium complex are involved in the catalytic cycle as shown in Scheme 1a [4]. Since the postulate of these bifunctional ruthenium based-molecular catalysts with cooperating amine/amido ligands has been proposed, the theoretical study also evoked many chemists' interest [5].

In recent years, continuous efforts have been made to develop new catalytic systems for the ATH reactions with the archetypal catalyst to improve the efficiency in terms of activity [6], selectivity [7], substrate scope [8] and practicability [9–11]. To address the latter issue, supported catalysts [10,11] have inherently operational and economical advantages: facilitating the separation from reaction mixtures, easy recovery and reuse of the expensive but always toxic chiral transition-metal catalysts. Amongst them, dendritic catalysts have received special attention since they have the potential to combine both the advantages of homogeneous and heterogeneous catalysts in a single system [12]. However, in terms of catalyst activity and reusability, dendritic catalysts [11] cannot outperform other types of catalysts immobilized on inorganic materials, such as silica [10b,d,f]. Compared to inorganic materials, the normal dendrimer [13] is now viewed as a "flexible" carrier [11,14] in supported catalysts. Herein we reveal a "semi-rigid" fluorinated dendrimer [15] as a functional carrier [16] in ruthenium(II) catalyst for asymmetric transfer hydrogenation reactions.

As a part of our own program of studies, we have recently developed a fluorinated dendritic chiral mono-*N*-tosylated 1,2-diphenylethylenediamine ruthenium complex (Ru-G-2-F, see Scheme 1b) for the asymmetric transfer hydrogenation of ketones in aqueous medium [17]. Compared to other dendritic catalysts

* Corresponding authors. Tel.: +86 21 63846590; fax: +86 2164154900.
E-mail addresses: weiweiwang@shsmu.edu.cn (W.-W. Wang), zmli@fudan.edu.cn (Z.-M. Li).

http://dx.doi.org/10.1016/j.molcata.2014.02.030
1381-1169/

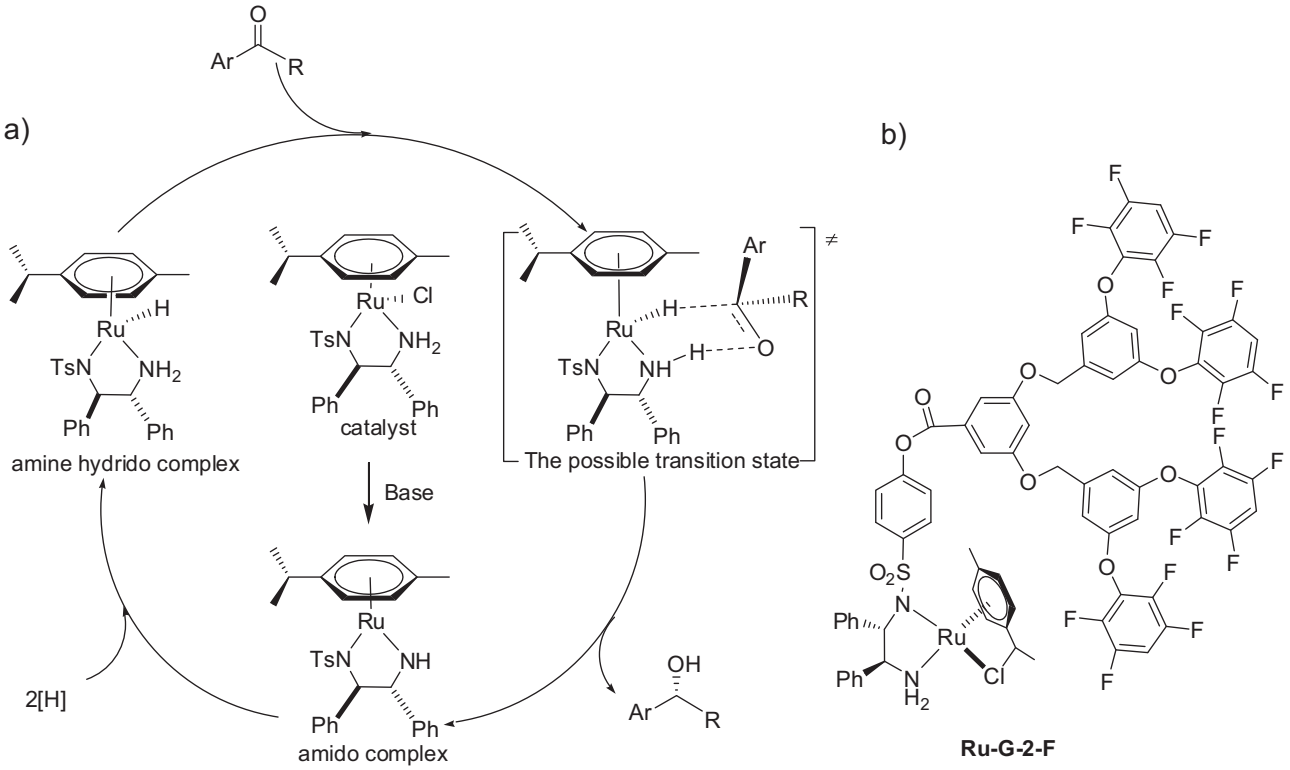

Scheme 1. (a) Concerted hydrogen transfer mechanism for ATH of ketones catalyzed by Ru–TsDPEN catalyst. (b) Structure of fluorinated dendritic chiral mono-*N*-tosylated 1,2-diphenylethylenediamine ruthenium complex Ru-H-G-2-F.

[11], this new well-defined catalyst leads to reactions with high activity and excellent recycling ability up to twenty-six times.

Although we have shown that Ru-G-2-F complex was highly stabilized and efficient with performances far surpassing those obtained from other types of dendritic and immobilized catalysts [10,12], little is known about the nature of the active sites and in particular what the real role of the fluorinated dendrimers play in affecting the activity and the stability of the Ru catalytic sites.

In the present work, detailed experiments combined with theoretical computation have been carried out to unravel the characteristic of fluorinated dendrimers and their role on the high activity and stability of our catalyst. First, a series of catalysts were synthesized, and the catalytic activities and reusabilities were evaluated including those at high temperatures [6i]. We were pleasingly to disclose that Ru-G-2-F exhibited unprecedented recycling ability up to twenty-three times even at 80 °C with enhanced activity and unaltered enantioselectivity. A novel stabilization pattern of the catalyst is proposed: the existence of fluorine atoms [15g] leads to considerable intramolecular weak interactions such as π–π stacking [15g,18] and hydrogen bonding [15g,19] interactions, which make the dendritic segment occur as a relatively rigid status in the catalyst and hence assists the performance of the catalytic center.

2. Experimental

2.1. Generals

The ^{1}H NMR, ^{13}C NMR and ^{19}F NMR spectra were acquired in $CDCl_3$ as solvent on a Bruker DMX 500 or a JEOL ECA-400 spectrometer. The chemical shifts (δ) are expressed in ppm (parts per million) relative to TMS (CF_3COOH, for ^{19}F NMR). Spin-spin coupling constants (J) were measured directly from the spectra and were given in Hz. Exact mass spectra (HR-MS) were recorded on IonSpec 4.7 Tesla FTMS. GC–MS spectra were recorded on PE 680-SQ8T (GC analysis: HP-5ms 30 m × 0.25 m × 0.25 μm, T = 50–280 °C, 1.0 mL/min). IR spectra were obtained on an Avatar 360 FT-IR spectrometer. Optical rotations were measured on an Autopol IV automatic polarimeter. Enantiomeric excesses were determined on GC analysis and HPLC analysis. The reactions were monitored by thin layer chromatography coated with silica gel. All solvents were purified and dried by standard procedures and kept over a suitable drying agent prior to use. Unless otherwise noted, all reagents were purchased from commercial sources and were used without further purification.

2.2. General procedure for the transfer hydrogenation reactions

Synthesis of pre-catalyst ***Ru-G-n-F*** *(n = 1, 2, 2′, 3)*: $[RuCl_2(p\text{-cymene})]_2$ (3.0 mg, 0.005 mmol), ligand **G-n-F** (n = 1, 2, 2′, 3) (0.011 mmol) and Et_3N (2.0 mg, 0.02 mmol) was dissolved in 1 mL of CH_2Cl_2. After the solution was stirred at 35 °C for 10 h, the solvent was removed to provide **Ru-G-n-F** (n = 1, 2, 2′, 3) as a crude solid. The crude product **Ru-G-n-F** (n = 1, 2, 2′, 3) was used directly in the following asymmetric transfer hydrogenation reactions as the catalyst.

Reduction of ketones using catalyst ***Ru-G-n-F*** *(n = 1, 2, 2′, 3):* The catalyst **Ru-G-n-F** (n = 1, 2, 2′, 3) (0.01 mmol), CH_2Cl_2 (0.5 mL), ketone (1.0 mmol) and TBAI (tetrabutylammonium iodide, 185 mg, 0.5 mmol) were added in 5 M liquor of HCO_2Na (6 mL), and the mixture was stirred at the corresponding temperature (10 °C, 40 °C, 60 °C, 80 °C) under nitrogen for a certain period of time. After the reaction was completed (monitored by TLC), the reaction mixture was extracted with ethyl acetate (20 mL). The organic phase was dried over anhydrous Na_2SO_4 and concentrated under reduced pressure. The product was purified by flash chromatography.

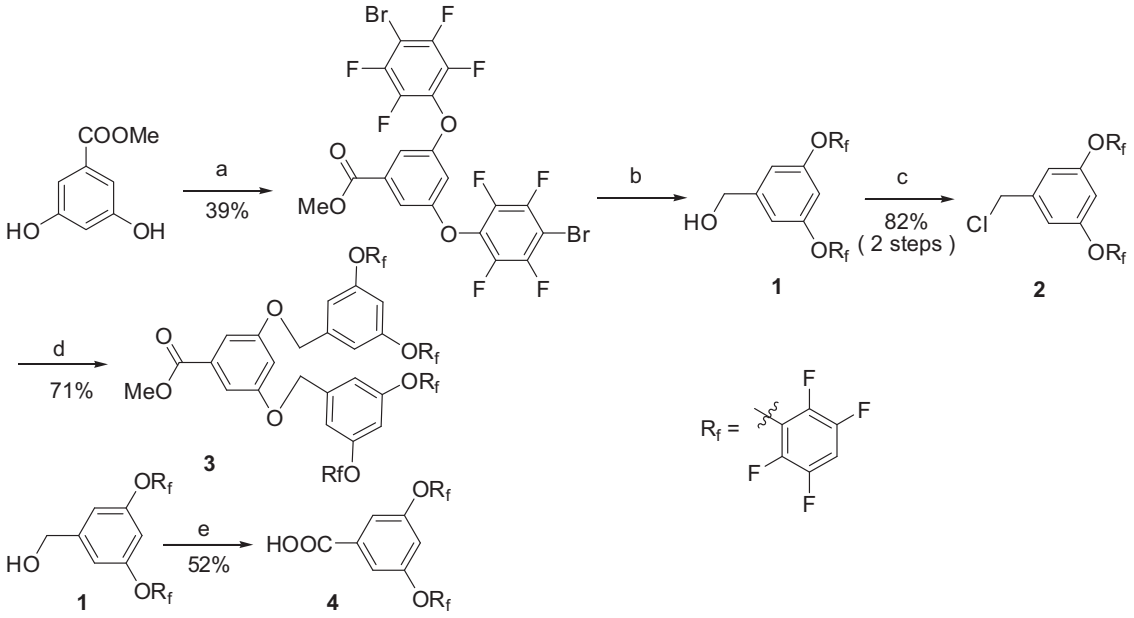

Scheme 2. Preparation of the second-generation fluorinated dendrimer **3** and first-generation fluorinated dendrimer **4**. *Reagents and conditions:* (a) Bromopentafluorobenzene, NaH, DMF.(b) $LiAlH_4$, THF. (c) PPh_3, CCl_4, acetonitrile. (d) Methyl 3,5-dihydroxybenzoate, K_2CO_3, TBAI, acetone. (e) Jones reagent, acetone.

2.3. Recovery and reuse of the catalyst

$[RuCl_2(p\text{-cymene})]_2$ (3.0 mg, 0.005 mmol), ligand **G-n-F** (n = 1, 2, 2′, 3) (0.011 mmol) and Et_3N (2.0 mg, 0.020 mmol) was dissolved in 0.5 mL of CH_2Cl_2. After the solution was stirred at 35 °C for 10 h, the mixture of ketone (1.0 mmol) and TBAI (tetrabutylammonium iodide, 185 mg, 0.5 mmol) in 5 M liquor of HCO_2Na (6 mL) was added. The mixture was stirred at the corresponding temperature (40 °C and 80 °C) under nitrogen for a certain period of time. After the reaction was completed (monitored by TLC), hexane (20 mL) were added to the reaction mixture and the catalyst began to precipitate from solution. The organic phase was removed by using a syringe, and washed with saturated brine (20 mL) and then dried (Na_2SO_4). The solvent was removed, and the product was purified by flash chromatography on silica gel to afford pure alcohol product.

For the next run of the reduction to be conducted, 1 equiv. HCO_2H (0.1 mL, 10 M) was added to adjust the pH value. The new reduction was started by feeding another portion of ketone (1.0 mmol) in 0.5 mL of CH_2Cl_2. The solution was allowed to react and the same workup procedure was used as mentioned above. Subsequent runs were performed in the same manner as the second.

3. Results and discussion

3.1. Synthesis of the fluorinated dendritic chiral ligands

Considering the structure of G-2-F [17], fluorinated dendritic chiral ligands G-1-F and G-3-F were designed and synthesized. As shown in Scheme 2, the second-generation fluorinated dendrimer **3** was obtained in a four-step sequence according to our previously reported method [17]. The first-generation fluorinated dendrimer **4** was prepared by oxidation of the benzyl alcohol **1** with Jones reagent.

However, the attempt to synthesize the third-generation fluorinated dendrimer **7** was proved to be unsuccessful. We found that the reduction of dendrimer **3** to alcohol analog **5** was very sluggish by using a diversity of reducing reagents including $LiAlH_4$. This result persuaded us to develop an alternative route for accessing larger fluorinated dendrimer.

As illustrated in Scheme 3, the intermediate **5** was prepared from halogenide **2** and 3,5-dihydroxylbenzyl alcohol with an acceptable yield, which was adopted by Ueda et al. [20]. It is worthy of comment that the halogenation conversion of alcohol **5** to halogenide **6** could be greatly promoted by addition of TBAI (tetrabutylammonium iodide). Finally, treatment of halogenide **6** with 3,5-dihydroxylbenzyl methyl ester under basic condition afforded dendrimer **7**.

The fluorinated dendrimer **4** and **7** were converted to their acid derivatives by saponification respectively. Finally, the fluorinated dendritic chiral ligands G-1-F and G-3-F were obtained by coupling the acid groups of the corresponding fluorinated dendrimers with the modified chiral ligand **8** [21] under the conditions of EDC/DMAP and consecutive deprotection of the Boci-group (Scheme 4).

3.2. Catalyst application and recovery study

With the fluorinated dendritic chiral ligands in hand, their performance was evaluated for use as ruthenium complex in the asymmetric transfer hydrogenation reactions of ketones. According to our previously established procedure [17], the reaction was performed under aqueous reaction conditions using HCO_2Na as a hydrogen source. The pre-catalyst was generated by reaction of the ligands with $[RuCl_2(p\text{-cymene})]_2$ in CH_2Cl_2 at 35 °C for 1 h with Et_3N as a base.

The transfer hydrogenation of acetophenone in aqueous media was employed as the benchmark reaction (Table 1). All the three catalysts displayed high catalytic activity and good enantioselectivity. Compared to Ru-G-2-F (entry 2, [17]), an enhanced reactivity was observed for Ru-G-1-F (entry 1), but Ru-G-3-F (entry 3) was less active with much longer reaction time due to its bigger dendritic backbone. This may be explained by the steric hindrance and the semi surrounding structure of the dendrimer [6i], which counterbalance the activity of the real catalysts [11a,d].

One of the most important motivations to design the fluorinated dendritic catalysts was to facilitate catalyst/product separation and recover the catalyst. Thus, the reusability of the catalysts was

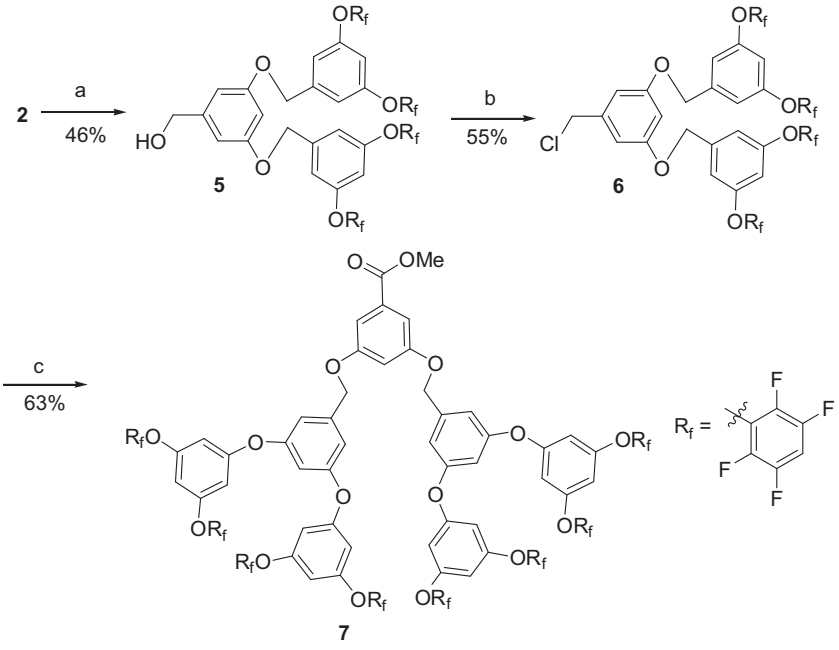

Scheme 3. Preparation of third generation fluorinated dendrimer **7**. *Reagents and conditions:* (a) 3,5-Dihydroxylbenzyl alcohol, K_2CO_3, NMP. (b) PPh_3, CCl_4, TBAI, acetonitrile. (d) Methyl 3,5-dihydroxybenzoate, K_2CO_3, TBAI, acetone.

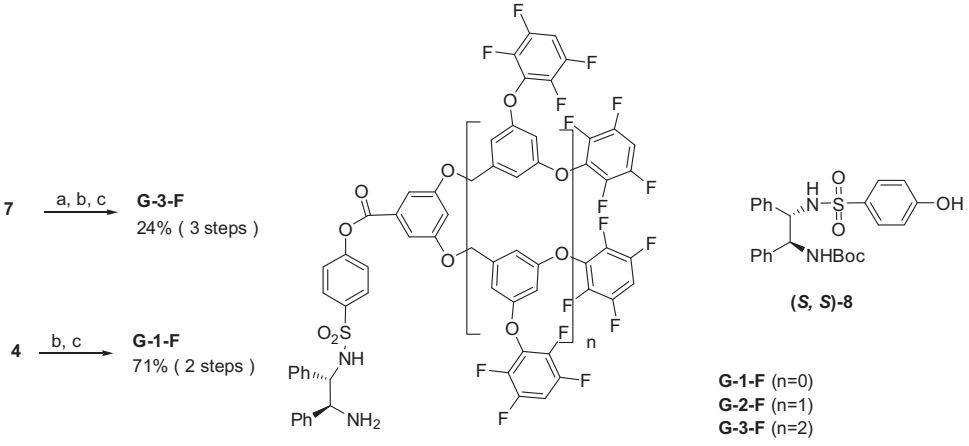

Scheme 4. Synthesis of fluorinated dendritic chiral ligands **G-1-F** and **G-3-F**. *Reagents and conditions:* (a) NaOH, H_2O. (b) (*S,S*)-**8**, EDC, DMAP, CH_2Cl_2. (c) TFA, CH_2Cl_2.

Table 1
Asymmetric transfer hydrogenation of acetophenone catalyzed by Ru-G-n-F (*n* = 1, 2, 3).[a]

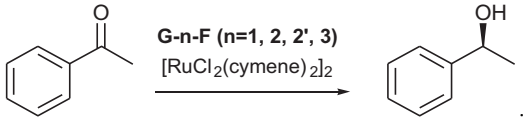

Entry	Ligand	*T* (°C)	*t* (h)	Conv. (%)[b]	ee (%)[c]
1	G-1-F	40	3	>99	97 (*S*)
2	G-2-F	40	4	>99	97 (*S*)
3	G-3-F	40	7	>99	94 (*S*)

[a] The reactions were carried out in 5 M liquor of HCO_2Na (6 mL) and CH_2Cl_2 (0.5 mL) with TBAI (0.5 equiv.) under a nitrogen atmosphere, S/C = 100. The configuration of the ligands was assigned as *S,S*.
[b] Yield of isolated product after flash chromatography.
[c] Determined by GC analysis using a CHIRALSIL-DEX-CB capillary column and HPLC analysis using a Daicel Chiralcel OB-H column. The configuration of the alcohol was assigned as *S*.

investigated at 40 °C with an S/C ratio of 100/1. After completion of the reaction, hexane was added to precipitate the catalyst. For the next run to be conducted, 1 equiv. of HCO_2H was added to adjust the pH.

In our previously reported results [17], Ru-G-2-F behaved excellently and can be reused more than twenty-six runs with no significant decline both in selectivity and activity (Fig. 1b). Compared to Ru-G-2-F, Ru-G-1-F almost lost the recycling ability just as unmodified Ru-TsDPEN (Fig. 1a). Ru-G-3-F was evidently inferior, which can be reused only nine runs (Fig. 1c). However, this result still outperforms other types of dendritic catalysts. [11] And this reveals that the structure of the fluorinated dendrimer plays an important role in the stability of the catalyst, and the second generation fluorinated dendrimer is the most suitable carrier for ATH catalyst.

3.3. NMR and computation study

To get deep insight in the nature of our dendrimer ruthenium catalyst and in particular the role of the ancillary dendrimer

fragment on the catalyst, the NMR and **c**omputational study were performed with our catalyst and the corresponding fluorinated dendrimer. As described above, **Ru-G-2-F** is the most efficient catalyst in our work, we therefore selected **Ru-G-2-F** and the second-generation fluorinated dendrimer **3** as the research model.

In the NMR spectra of the dendrimer **3** at 25 °C (Fig. 2c), there are two peaks corresponding to the benzyl protons: a main peak (δ = 5.092) and a tiny peak (δ = 5.117) beside it. This abnormal phenomenon is also discernible in the ^{1}H NMR spectra of G-2-F (Fig. 3a) and Ru-G-2-F (Fig. 3b). Moreover, in the NMR spectra of G-2-F, the area of the down-field peak increased apparently compared with that of the dendrimer. The ratio of the two peak areas in lower field to that in upper field in G-2-F is about 1:2, larger than that in the dendrimer. In Ru-G-2-F, the ratio is further increased to 1:1. An NMR spectrum represents the statistical result from the thermodynamic and kinetic effect. Thus we assume that there should be a thermodynamic stable conformer corresponding to the tiny peak, and the conversion barrier between other conformers and this conformer is substantial. So we first set out to locate the most stable conformer of dendrimer **3**.

On the basis that MM [22] force field can give reasonable conformations and energetics compared to the *ab initio* results, we first carried out a Monte Carlo [23] conformational search for fluorinated dendrimer **3** using MM force field with the Hyperchem program [24]. Totally, 5000 structures were optimized during the conformational search, and conformations within 12 kcal/mol with respect to the most stable conformation were accumulated. To ensure that all the conformers in the low-energy area were obtained, another conformational search starting with the lowest energy conformer that had been found in the first run was carried out and the same result was obtained. On the basis of the conformational search results, 30 lowest energy conformers (within about 4.0 kcal/mol relative to the global minimum) were optimized with PM6 method, in which the 10 lowest energy conformers (within about 2.3 kcal/mol relative to the global minimum) were optimized with the M062X/6-31G(d) [25] method of computation using the GAUSSIAN09 programm [26].

Our computation results indicate that the introduction of fluorine atoms confers certain scaffold rigidity. The most stable conformer of the 10 lowest energy conformers features a very rigid structure *via intra*molecular hydrogen bonding (C–H···F and C–H···O hydrogen bonds) and π–π stacking interactions between aromatic rings including fluorinated phenyl rings (see Figure S1 and Table S1). This hydrogen bond influence is unique compared to other non-fluorinated dendrimers [13]. Computations reveal that there is a three-center hydrogen bond in this conformer, which exists between F, O atoms of a fluorinated phenyl and an H atom of the phenyl ring connected directly with the benzyl carbon, the distances of H···O and H···F are 2.21 and 2.58 Å, respectively (see Figure S1). Moreover, there is an interesting sandwich structure due to the π–π stacking interactions [27] between the three fluorinated phenyl rings (see Figure S1). Thus the rotations about the single bond are constrained. On the other hand, the shortest distance between the two aromatic rings connected directly with the two methylene carbons is only about 3.22 Å, while similar situations can not be found in other 9 stable conformers (Fig. 2b). The short distances and the strong π–π stacking interactions in the most stable conformer enhance the induced magnetic field of

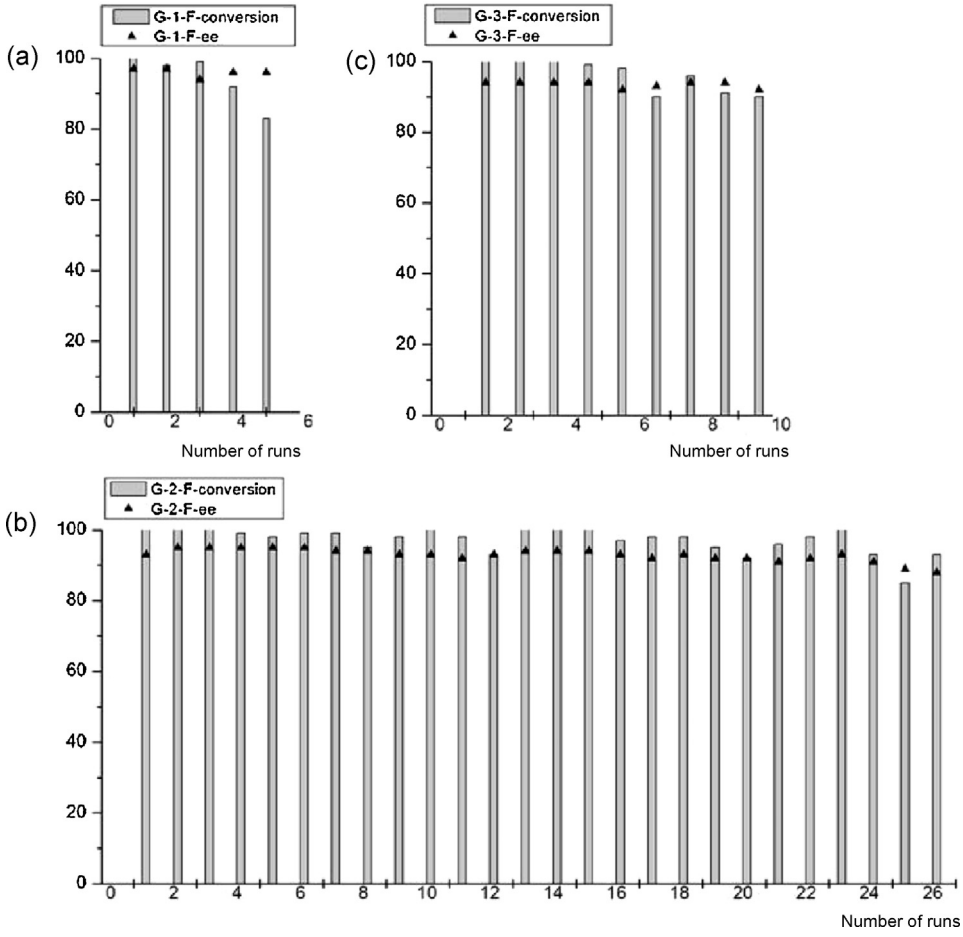

Fig. 1. Graph of conversion, ee *vs.* run numbers for the reduction of acetophenone with Ru-G-1-F (a), Ru-G-2-F [17] (b) and Ru-G-3-F (c) in water at 40 °C.

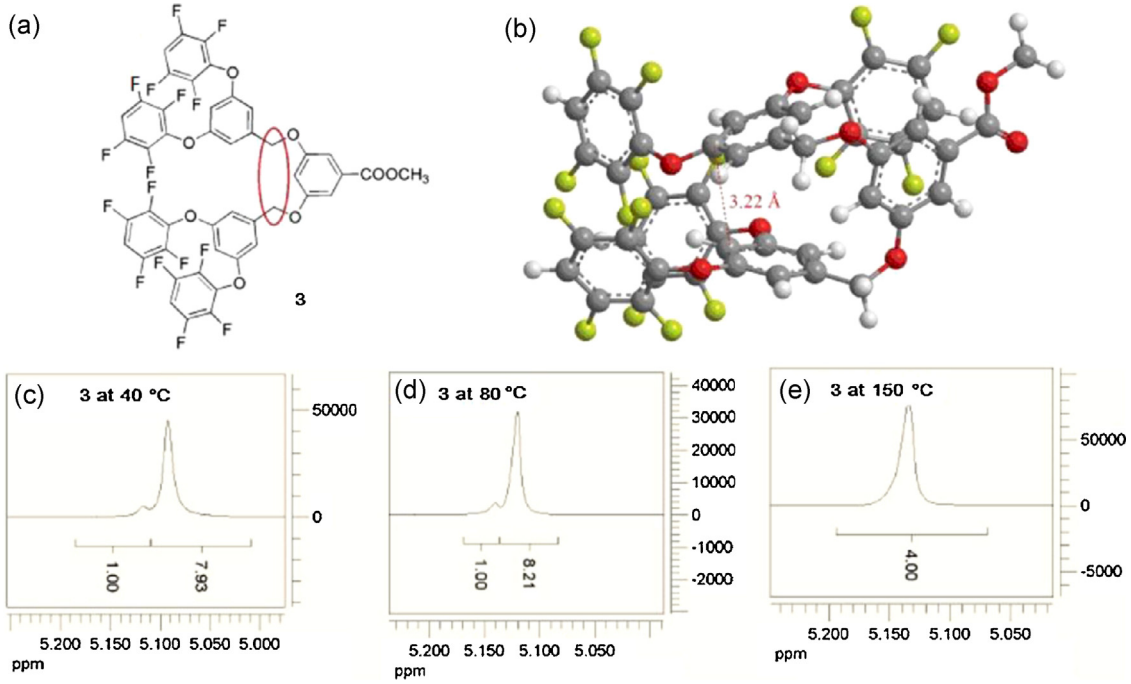

Fig. 2. (a) Molecular structure of the fluorinated dendrimer **3**. (b) Optimized structure of the global minimum of fluorinated dendrimer **3**. (c) ^{1}H NMR spectra of benzyl protons of **3**, 25 °C. (d) 80 °C. (e) 150 °C.

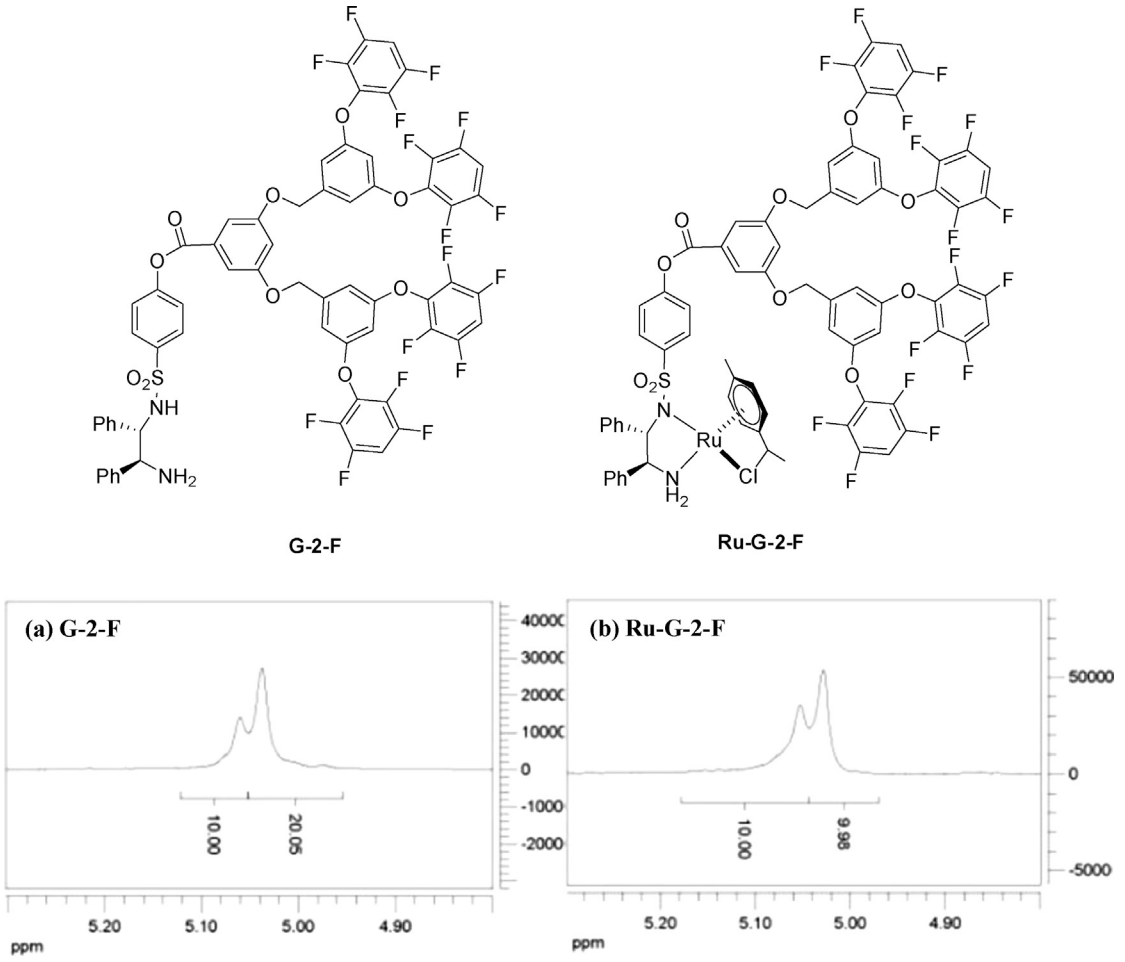

Fig. 3. ^{1}H NMR spectra of benzyl protons of (a) G-2-F, (b) Ru-G-2-F.

the phenyl π electrons, and consequently reinforce the deshielding of aryl protons and benzyl protons as well [28]. The tiny peak (δ = 5.117) beside the main peak (δ = 5.092) is attributed to the benzyl protons in the most stable conformer. Since one can only get the average environment of the protons in the NMR time-scale, the main peak at upper-field is attributed to the benzyl protons in other conformers of the dendrimer, in which the hydrogen bonding and π–π stacking interactions are less significant.

In the case of G-2-F and Ru-G-2-F, we assumed that the introduction of polar group such as amino group, more aromatic rings and rigid Ru segment can enhance the rigid character of G-2-F and Ru-G-2-F for more hydrogen bonding and π–π stacking interactions, and consequently stabilize the most stable conformers to more extent.

To test this assumption, we set about to explore the ligand G-2-F and the ruthenium catalyst Ru-G-2-F, based on the crystal structure of the ligand and ruthenium catalyst [4a]. Considering the computation cost, the dendrimer moiety was constrained to the structure of the lowest energy conformer of the original dendrimer (labeled with **A**), and the potential energy profiles were scanned along the three bonds of the ester unit between the dendrimer skeleton and the chiral diamine part (see Figure S2 and Figure S3). The structure of the ligand and the catalyst with the lowest energy in the scanned potential energy profiles were then located. Finally, the structures were optimized with the M062X method using 6-31G(d) basis set for the main group atoms and the SDD basis set for Ru atom [29]. To our gladness, the computation results agree well with our assumption: the conformer of G-2-F-A and Ru-G-2-F-A with the lowest energy are also rigid and the rotation of the dendrimer part turns to be more constrained, which are from more hydrogen bonding, π–π stacking interactions as well as the rigid Ru-based fragment. For instance, in G-2-F, one of the hydrogen of NH_2 and one hydrogen of phenyl ring connected directly with $CHNH_2$, can form a three-center hydrogen bond with one F atom of dendrimer part (see Figure S4) [30].

Following the same strategy, the second stable dendrimer (see Table S1–S2) was used to build the structure of G-2-F and Ru-G-2-F (labeled with **B**). The computation results exhibit that the most stable conformer of G-2-F-A and Ru-G-2-F-A can be more stabilized than G-2-F-B and Ru-G-2-F-B (see Figure S5 and Table S2). The difference between the free energies of G-2-F-A and G-2-F-B is 5.2 kcal/mol, obviously larger than that of the dendrimers (ΔG = 4.7 kcal/mol). These data predict that G-2-F content with the most stable dendrimer conformer structure is increased. For Ru-G-2-F, the ΔG of **A** and **B** is enlarged to 16.8 kcal/mol, suggesting that the rigid structure of Ru-G-2-F-A is more stabilized than Ru-G-2-F-B, and the rigid character of Ru-G-2-F becomes more pronounced.

Considering the computation cost, the interconversion transition state and barriers between conformers are not located. But on the basis of the previous computational results, we can deduce that hydrogen bonding and π–π stacking interactions contribute a lot to the barrier. On the other hand, variable-temperature NMR experiment can give us some clues about the barrier. In order to prove our prediction, the ^{1}H NMR experiments at 25, 80, 150 °C were performed. We can reasonably envision that, with the increase of the temperature, the remote *intra*molecular interactions such as π–π stacking and hydrogen bonding will decrease thus the tiny peak area declines. The experimental clearly verified our prediction. Though the tiny peak area at 80 °C does not change much as compared with that at 25 °C (Fig. 2d), it did disappear completely at 150 °C (Fig. 2e), indicating that the energy barrier separating the most stable conformer and other conformers is sizable but the molecules at 150 °C can surmount it freely. In view of the NMR experiments, we can also predict that 80 °C is a safe temperature for the catalyst, and the catalytic reaction temperature can be increased to 80 °C, which is advantageous for performing the AHT reactions.

Similarly, **c**omputational study from the same strategy as Ru-G-2-F, is performed with the hydride intermediate Ru-H-G-2-F (Fig. 4). To our satisfaction the calculation results demonstrate the existence of a similar rigid structure in Ru-H-G-2-F [4,5]. The ΔG between Ru-H-G-2-F-A and Ru-H-G-2-F-B is 17.1 kcal/mol, larger than that of Ru-G-2-F (ΔG = 16.8 kcal/mol). This value verified that Ru-H-G-2-F-A is more stabilized as compared to Ru-H-G-2-F-B when Ru-G-2-F is converted to Ru-H-G-2-F. Besides, it is worth noting that there is a three-center hydrogen-bond in the hydride intermediate, which is between one of the F atoms in the dendrimer part, an H atom on NH_2, and an H atom on the phenyl ring connected directly with $CHNH_2$ (Fig. 4). The distance between the F atom and the H atom on NH_2 is 2.13 Å, and the bond angle of N–H···F is 158.2°. These data means that this hydrogen bond is relatively strong. Moreover, the hydrogen atom is one member in the six-membered ring in the transition structure (Scheme 1a). Thus, the higher stability of our catalyst may result from this strong hydrogen bond to a large extent: the rigid fluorinated dendrimer part participates in the catalytic cycle *via* this hydrogen bonding and stabilizes the amine hydrido complex intermediate. This concept has been proved in Xiao's work [5b], in which the solvent water forms a hydrogen bond to the ketone oxygen in the transition state of hydrogen transfer. Thus, the dendrimer size may play an important role in affecting the catalyst efficiency (See Figure S6).

From the above discussion, we can come to the following conclusions: first, due to the stable rigid conformation of the fluorinated-dendrimer catalyst, it is easy to precipitate out the catalyst from the reaction system, similar to the inorganic carrier supported catalyst. Second, for the hydrido(amine)ruthenium complex intermediate Ru-H-G-2-F (Fig. 1b), the hydrogen atom in the hydrogen bond N–H···F is one member of the six-membered ring in the catalytic transition structure, which stabilizes the hydride intermediate and thus elongate the catalytic lifetime and rendering much better recycling performance than other types of supported catalyst such as the inorganic carrier supported ones.

3.4. Design, synthesis and application of new catalyst

In order to prove our mechanistic assumption, a new chiral ligand G-2′-F was designed and prepared. As shown in Scheme 5, compound **9** was readily assembled from halogenide **2**, then the chiral ligand G-2′-F was prepared according to our previously established method. The structure of compound **9**, which contains half size of the second generation fluorinated dendrimer **3**, is asymmetric in the structure, different from the common dendrimer molecules. The corresponding catalyst Ru-G-2′-F contains only two fluorinated phenyl rings as in Ru-G-1-F, but has the same distance between the terminus of the fluorinated carrier part and the Ru catalytic sites as in Ru-G-2-F. Based on our theoretical computation results, the F atoms in catalyst Ru-G-2′-F (in the end of carrier part) can influence the performance of the Ru catalytic sites in the hydrido(amine) intermediate as in Ru-G-2-F, thus extend the lifetime and enhance the recycling ability of the catalyst.

The experimental results of Ru-G-2′-F verified our assumption. The asymmetric transfer hydrogenation of acetophenone in aqueous media afforded 99% conversion and 96% ee in 2 h at 40 °C. As expected, the recycling of the Ru-G-2′-F at 40 °C proved to be quite satisfactory. As shown in Fig. 5, the catalyst can be reused more than fifteen times. Even in the 15th run, the reaction also afforded 91% conversion and 95% ee in 18 h. This result outperforms Ru-G-1-F (5 runs) and even Ru-G-3-F (9 runs).

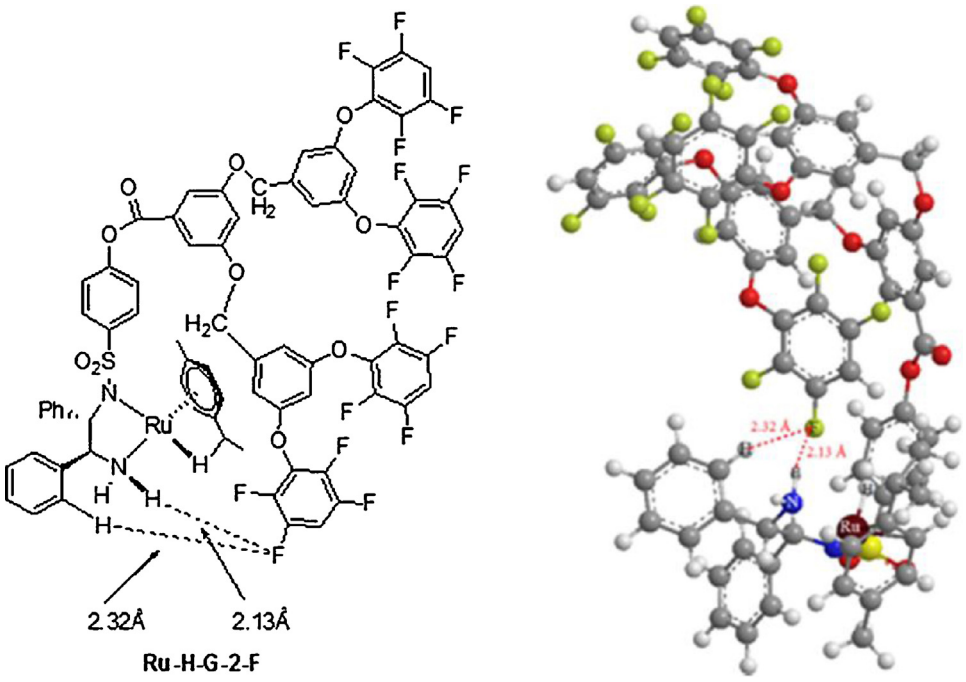

Fig. 4. Molecular structure (left) and optimized structure (right) of the lowest energy conformer in the scanned potential energy profiles of Ru-H-G-2-F.

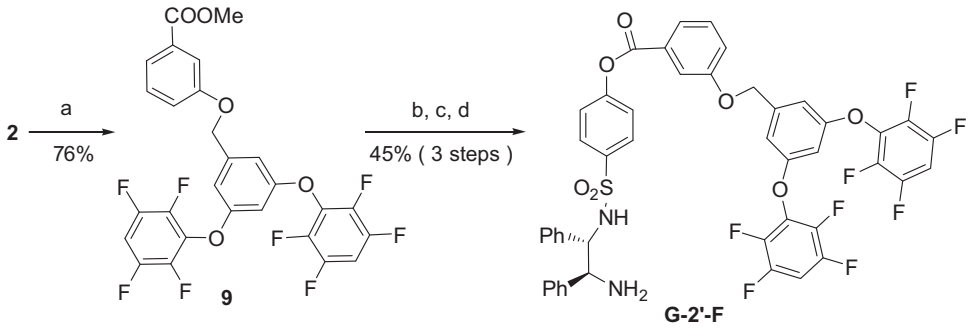

Scheme 5. Synthesis of chiral ligands G-2′-F. *Reagents and conditions:* (a) Methyl 3,5-dihydroxybenzoate, K_2CO_3, TBAI, acetone. (b) NaOH, H_2O. (c) (*S*,*S*)-**8**, EDC, DMAP, CH_2Cl_2. (d) TFA, CH_2Cl_2.

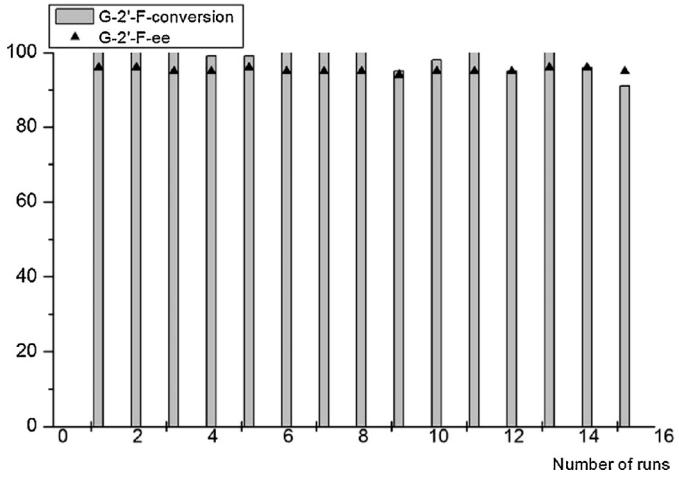

Fig. 5. Graph of conversion, *ee vs.* run numbers for the reduction of acetophenone with Ru-G-2′-F in water at 40 °C.

3.5. Catalyst application at high reaction temperature

Although we have shown that Ru-G-2-F complex provides high enantioselectivity and outstanding recycling ability, the improvement in activity nearly remained unchanged as compared to the unmodified system. As mentioned above, the conversion barrier from the most stable conformer to other conformers is comparable and the temperature of 80 °C is a possible safe temperature to promote the transfer hydrogen reaction without significant change in the catalyst conformation (See Figure S7), thus accelerating the reaction rate. A series of temperature gradients (10 °C, 60 °C, 80 °C) were investigated with Ru-G-2-F and the results are summarized in Table 2. Faster rates were obtained at higher temperatures without prominent loss in enantioselectivity (entry 1 *vs.* 2). At 80 °C, the reaction time was reduced to 25 min in 96% ee (entry 3). The catalyst also performed quit well to afford equal enantioselectivity at a lower catalyst dosage of S/C = 1000, yet a longer reaction time was required (entry 5).

Encouraged by these results, we extended this protocol to a set of substituted acetophenones **11–15** and uniformly high enantioselectivities were obtained (entries 5–9). All of the tested ketones were successfully reduced within a few minutes with more than 99% conversion at 80 °C. Compared to the low temperature

Table 2
Asymmetric transfer hydrogenation of ketones catalyzed by Ru-G-n-F (n = 1, 2′, 2, 3).[a]

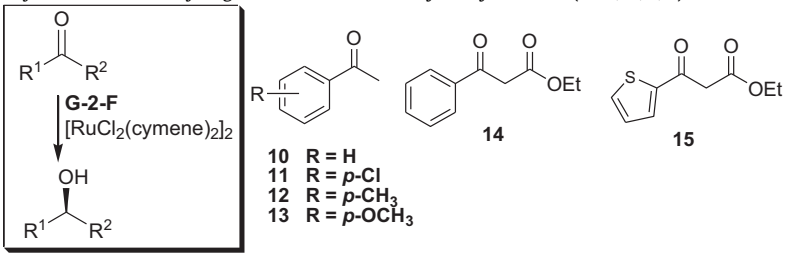

Entry	Ketone	Ligand	Tmep. (°C)	Time (h)	Conv. (%)[b]	ee (%)[c]
1	10	G-2-F	10	8	>99	98 (S)
2	10	G-2-F	60	1.5	>99	95 (*S*)
3	10	G-2-F	80	0.4	>99	96 (*S*)
4	10	G-2′-F	80	0.5	>99	94 (*S*)
5	10[d]	G-2-F	80	5	97	96 (*S*)
6	12	G-2-F	80	0.2	>99	94 (*S*)
7	12	G-2-F	80	1.1	>99	96 (*S*)
8	13	G-2-F	80	0.9	>99	95 (*S*)
9	14	G-2-F	80	0.2	>99	94 (*S*)[e]
10	15	G-2-F	80	0.3	>99	96 (*S*)[e]

[a] The reactions were carried out in 5 M liquor of HCO_2Na (6 mL) and CH_2Cl_2 (0.5 mL) with TBAI (0.5 equiv.) under a nitrogen atmosphere, S/C = 100. The configuration of the ligands was assigned to be *S,S*.
[b] Isolated yield by flash chromatography.
[c] Determined by GC analysis using a CHIRALSIL-DEX-CB capillary column and HPLC analysis using a Daicel Chiralcel OB-H column. The configuration of the alcohol was assigned as *S*.
[d] The reaction with S/C = 1000.
[e] Determined by HPLC analysis using a Daicel Chiralcel OD column. The configuration of the alcohol was assigned as *S*.

conditions [17], the deterioration of enantiomeric purity of the products was generally less than 1%. The reduction of β-ketoester **14** led to a >99% conversion in 94% ee in only 10 minutes (entry 8). In comparison, the same reaction performed at 40 °C was sluggish with only 92% ee [17]. Particularly noteworthy is that the thiophene substrate **15** was also successfully reduced in 99% yield and 96% ee within only 20 minutes, leading to the corresponding (*S*)-β-hydroxy carboxylic ester, which serves as the key synthetic intermediate for the antidepressant drug duloxetine [21,31].

Next, Ru-G-2-F was applied to investigate the catalyst reusability at 80 °C. To our delight, the catalyst can be reused more than twenty-three times with no significant decline both in selectivity and activity (Fig. 6a). As shown in Fig. 6, during the initial recycling period (runs 1–10), excellent conversion and enantioselectivity were obtained with no extension of the reaction time. The *ee* values remained almost unchanged until the last run (23rd run, 82% conversion and 93% *ee*, in 180 minutes). No appreciable ruthenium leaching into the product was observed as proved by an ICP analysis [32]. These excellent experimental results with high enantioselectivity and efficiency can be maintained at 80 °C.

Finally, we also attempted to use Ru-G-2′-F at high temperature. Although Ru-G-2′-F was proved to work well at 80 °C (Table 2, entry

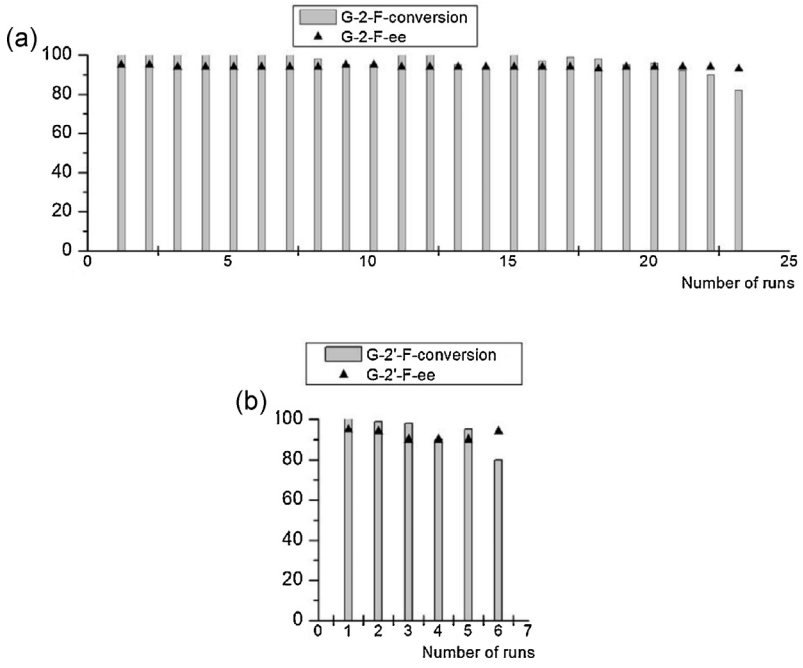

Fig. 6. Graph of conversion, *ee vs.* run numbers for the reduction of acetophenone with (a) Ru-G-2-F and (b) Ru-G-2′-F in water at 80 °C.

4), the recycling ability of the catalyst was considerably dissatisfactory in comparison to that of Ru-G-2-F. The catalyst could only be reused for no more than six times (Fig. 6b). We hypothesized that this is due to the imperfect π–π stacking interactions of the carrier part moiety with less number of aromatic rings.

4. Conclusion

In conclusion, we have demonstrated that the fluorinated dendrimer plays a vital role in the catalyst system, which has a well-defined semi-rigid structure. Both of the theoretical analyses and experimental examination revealed that introduction of an appropriate fluorinated dendrimer can influences the performance of the Ru catalytic sites in the hydrido(amine)ruthenium complex intermediate, thus extend the lifetime and enhance the recycling performance of the catalyst. This strategy has been employed for designing and realization of a novel Ru(II)-complex catalyst Ru-G-2′-F, which exhibits obviously improved recycling ability up to fifteen times. Significantly enhanced activity, high enantioselectivity and outstanding recycling ability have been achieved at high reaction temperature with Ru-G-2-F. We believe that the fluorinated dendrited ligands offer a conceptually new prototype for the design of related bifunctional catalysts with cooperating amine-amido ligands, and also open new perspectives in the application of fluorinated dendrimer as a functional carrier.

Acknowledgments

Financial support from the National Natural Science Foundation of China (NO. 21102019) are gratefully acknowledged.

Appendix A. Supplementary data

Supplementary material related to this article can be found, in the online version, at http://dx.doi.org/10.1016/j.molcata.2014.02.030.

References

[1] (a) R. Noyori, Asymmetric Catalysis in Organic Synthesis, John Wiley & Sons, New York, 1994;
(b) R. Noyori, S. Hashiguchi, Acc. Chem. Res. 30 (1997) 97;
(c) T. Ikariya, A. Blacker, J. Acc. Chem. Res. 40 (2007) 1300;
(d) X.-F. Wu, J.-L. Xiao, Chem. Commun. (2007) 2449.
[2] (a) S. Hashiguchi, A. Fujii, J. Takehara, T. Ikariya, R. Noyori, J. Am. Chem. Soc. 117 (1995) 7562;
(b) A. Fujii, S. Hashiguchi, N. Uemastu, T. Ikariya, R. Noyori, J. Am. Chem. Soc. 118 (1996) 2521;
(c) N. Uematsu, A. Fujii, S. Hashiguchi, T. Ikariya, R. Noyori, J. Am. Chem. Soc. 118 (1996) 4916.
[3] (a) S. Ogo, N. Makihara, Y. Watanabe, Organometallics 18 (1999) 5470;
(b) X.-F. Wu, X.-G. Li, W. Hems, F. King, J.-L. Xiao, Org. Biomol. Chem. 2 (2004) 1818.
[4] (a) K.-J. Haack, S. Hashiguchi, A. Fujii, T. Ikariya, R. Noyori, Angew. Chem., Int. Ed. 36 (1997) 285;
(b) R. Noyori, M. Yamakawa, S. Hashiguchi, J. Org. Chem. 66 (2001) 7931.
[5] (a) A. Hayes, G. Clarkson, M. Wills, Tetrahedron: Asymmetry 15 (2004) 2079;
(b) X.-F. Wu, X.-H. Li, A. Zanotti-Gerosa, A. Pettman, J. Liu, A.J. Mills, J.-L. Xiao, Chem. Eur. J. 14 (2008) 2209;
(c) X.-F. Wu, J. Liu, D.D. Tommaso, A.J. Iggo, C.R.A. Catlow, J. Bacsa, J.-L. Xiao, Chem. Eur. J. 14 (2008) 7699;
(d) J.E.D. Martins, G.J. Clarkson, M. Wills, Org. Lett. 11 (2009) 847;
(e) P.A. Dub, T. Ikariya, J. Am. Chem. Soc. 135 (2013) 2604.
[6] (a) C. Bubert, J. Blacker, S.M. Brown, J. Crosby, S. Fitzjohn, J.P. Muxworthy, T. Thorpe, J.M.J. Williams, Tetrahedron Lett. 42 (2001) 4037;
(b) T. Thorpe, J. Blacker, S.M. Brown, C. Bubert, J. Crosby, S. Fitzjohn, J.P. Muxworthy, J.M.J. Williams, Tetrahedron Lett. 42 (2001) 4041;
(c) D. Sterk, M.S. Stephan, B. Mohar, Tetrahedron: Asymmetry 13 (2002) 2605;
(d) Y.-P. Ma, H. Liu, L. Chen, X. Cui, J. Zhu, J.-G. Deng, Org. Lett. 5 (2003) 2103;
(e) J. Hannedouche, G.J. Clarkson, M. Wills, J. Am. Chem. Soc. 126 (2004) 986;
(f) X.-F. Wu, X.-G. Li, F. King, J.-L. Xiao, Angew. Chem., Int. Ed. 44 (2005) 3407;
(g) I. Kawasaki, K. Tsunoda, T. Tsuji, T. Yamaguchi, H. Shibuta, N. Uchida, M. Yamashita, S. Ohta, Chem. Commun. (2005) 2134;
(h) X.-F. Wu, D. Vinci, T. Ikariya, J.-L. Xiao, Chem. Commun. (2005) 4447;
(i) A.M. Hayes, D.J. Morris, G.J. Clarkson, M. Wills, J. Am. Chem. Soc. 127 (2005) 7318;
(j) F.K. Cheung, A.M. Hayes, J. Hannedouche, A.S.Y. Yin, M. Wills, J. Org. Chem. 70 (2005) 3188;
(k) D.S. Matharu, D.S. Morris, G.J. Clarkson, M. Wills, Chem. Commun. (2006) 3232;
(l) A.N. Cortez, G. Aguirre, M. Parra-Hake, R. Somanathan, Tetrahedron: Asymmetry 19 (2008) 1304;
(m) N. Vriamont, B. Govaerts, P. Grenouillet, C. Bellefon, O. Riant, Chem. Eur. J. 15 (2009) 6267;
(n) T.C. Johnson, W.G. Totty, M. Wills, Org. Lett. 14 (2012) 5230.
[7] (a) F. Wang, H. Liu, L.-F. Cun, J. Zhu, J.-G. Deng, Y.-Z. Jiang, J. Org. Chem. 70 (2005) 9424;
(b) D. Sterk, M.S. Stephan, B. Mohar, Org. Lett. 8 (2006) 5935;
(c) K. Ahlford, J. Lind, L. Maler, H. Adolfsson, Green Chem. 10 (2008) 832;
(d) I. Plantan, M. Stephan, U. Urleb, B. Mohar, Tetrahedron Lett. 50 (2009) 2676;
(e) W.-W. Wang, Z.-M. Li, W.-B. Mu, L. Su, Q.-R. Wang, Catal. Commun. 11 (2010) 480.
[8] (a) K. Murata, T. Ikariya, J. Org. Chem. 64 (1999) 2186;
(b) J.-M. Mao, D.C. Baker, Org. Lett. 1 (1999) 841;
(c) J.-S. Wu, F. Wang, Y.-P. Ma, L.-F. Cui, J. Zhu, J.-G. Deng, Chem. Commun. (2006) 1766;
(d) L. Li, J.-S. Wu, F. Wang, J. Liao, H. Zhang, C.-X. Lian, J. Zhu, J.-G. Deng, Green Chem. 9 (2007) 23.
[9] (a) T. Ohkuma, K. Tsutsumi, N. Utsumi, N. Arai, R. Noyori, K. Murata, Org. Lett. 9 (2007) 255;
(b) T. Ohkuma, N. Utsumi, M. Watanabe, K. Tsutsumi, N. Arai, K. Murata, Org. Lett. 9 (2007) 2565;
(c) C.-Q. Li, J.-L. Xiao, J. Am. Chem. Soc. 130 (2008) 13208;
(d) T. Touge, T. Hakamata, H. Nara, T. Kobayashi, N. Sayo, T. Saito, Y. Kayaki, T. Ikariya, J. Am. Chem. Soc. 133 (2011) 14960.
[10] (a) D.J. Bayston, C.B. Travers, M.E.C. Polywka, Tetrahedron: Asymmetry 9 (1998) 2015;
(b) P.-N. Liu, J.-G. Deng, Y.-Q. Tu, S.-H. Wang, Chem. Commun. (2004) 2070;
(c) X.-G. Li, X.-F. Wu, W.-P. Chen, F.E. Hancock, F. King, J.-L. Xiao, Org. Lett. 6 (2004) 3321;
(d) P.-N. Liu, P.-M. Gu, F. Wang, Y.-Q. Tu, Org. Lett. 6 (2004) 169;
(e) Y. Arakawa, N. Haraguchi, S. Itsuno, Tetrahedron Lett. 47 (2006) 3239;
(f) X.-H. Huang, J.Y. Ying, Chem. Commun. (2007) 1825;
(g) Y. Arakawa, A. Chiba, N. Haraguchi, S. Itsuno, Adv. Synth. Catal. 350 (2008) 2295;
(h) J.-T. Liu, Y.-G. Zou, Y.-N. Wu, X.-S. Li, A.S.C. Chan, Tetrahedron: Asymmetry 19 (2008) 832;
(i) N. Haraguchi, K. Tsuru, Y. Arakawa, S. Itsuno, Org. Biomol. Chem. 7 (2009) 69.
[11] (a) Y.-C. Chen, T.-F. Wu, J.-G. Deng, H. Liu, Y.-Z. Jiang, M.C.K. Choi, A.S.C. Chan, Chem. Commun. (2001) 1488;
(b) Y.-C. Chen, T.-F. Wu, J.-G. Deng, H. Liu, X. Cui, J. Zhu, Y.-Z. Jiang, M.C.K. Choi, A.S.C.J. Chan, Org. Chem. 67 (2002) 5301;
(c) Y.-C. Chen, T.-F. Wu, L. Jiang, J.-G. Deng, H. Liu, J. Zhu, Y.-Z. Jiang, J. Org. Chem. 70 (2005) 1006;
(d) L. Jiang, T.-F. Wu, Y.-C. Chen, J. Zhu, J.-G. Deng, Org. Biomol. Chem. 4 (2006) 3319.
[12] S.M. Grayson, J.M.J. Frechet, Chem. Rev. 101 (2001) 3819.
[13] (a) A.M. Caminade, C.O. Turrin, R. Laurent, A. Ouali, B. Delavaux-Nicot, Dendrimers. Towards Catalytic, Material and Biomedical Uses, Wiley, Chichester, UK, 2001;
(b) S. Campagna, P. Ceroni, F. Puntoriero, Designing Dendrimers;, Wiley, Hoboken, NJ, 2011;
(c) Y. Cheng, Dendrimer-based Drug Delivery Systems: from Theory to Practice;, Wiley, Hoboken, NJ, 2012.
[14] (a) S.-B. Garber, J.S. Kingsbury, B.L. Gray, A.H. Hoveyda, J. Am. Chem. Soc. 122 (2000) 8168;
(b) A.W. Kleij, R.A. Gossage, R.J.M.K. Gebbink, N. Brinkmann, E.J. Reijerse, U. Kragl, M. Lutz, A.L. Spek, G.J. Koten, Am. Chem. Soc. 122 (2000) 12112;
(c) A.-M. Caminade, J.-P. Majoral, Acc. Chem. Res. 37 (2004) 341;
(d) A.M. Caminade, J.P. Majoral, Prog. Polym. Sci. 30 (2005) 491;
(e) O. Rolland, C.O. Turrin, A.M. Caminade, J.P. Majoral, New J. Chem. 33 (2009) 1809.
[15] (a) V. Chechik, R.M. Crooks, J. Am. Chem. Soc. 122 (2000) 1243;
(b) M. Mager, S. Becke, H. Windisch, U. Denninger, Angew. Chem. Int. Ed. 40 (2001) 1898;
(c) L.K. Yeung, R.M. Crooks, Nano Lett. 1 (2001) 14;
(d) R. Roestler, B.J.N. Har, W.E. Piers, Organometallics 21 (2002) 4300;
(e) A.M. Caminade, C.O. Turrin, P. Sutra, J.P. Majoral, Curr. Opin. Colloid Interface Sci. 8 (2003) 282;
(f) D.A. Tomalia, Nat. Mater. 2 (2003) 711;
(g) P. Kirsch, Modern Fluroorganic Chemistry–Synthesis, Reactivity, Applications, Wiley-VCH Verlag GmbH & Co. KGaA, Weinheim, 2004;
(h) S.R. Punireddy, Y.K. Wai, N. Satyanarayana, S.K. Sinha, M.P. Srinivasan, Langmuir 23 (2007) 8299;
(i) Z.-X. Jiang, B.Y. Yu, J. Org. Chem. 75 (2010) 2044.
[16] M.K. Samantaray, J. Alauzun, D. Gajan, S. Kavitake, A. Mehdi, L. Veyre, M. Lelli, A.L. Lesage, L. Emsley, C. Coperet, J. Am. Chem. Soc. 135 (2013) 3193.
[17] W.-W. Wang, Q.-R. Wang, Chem. Commun. (2010) 4616.

[18] (a) P. Murray-Rust, W.C. Stallings, C.T. Monti, R.K. Preston, J.P. Glusker, J. Am. Chem. Soc. 105 (1983) 3206;
(b) C. Li, Y.-Y. Zhu, H.-P. Yi, C.-Z. Li, X.-K. Jiang, Z.-T. Li, Y.-H. Yu, Chem. Eur. J. 13 (2007) 9990.
[19] (a) C.A. Hunter, J.K.M. Sanders, J. Am. Chem. Soc. 112 (1990) 5525;
(b) S.E. Wheeler, K.N. Houk, J. Chem. Theory Comput. 5 (2009) 2301;
(c) S.A. Arnstein, D.C. Sherrill, Phys. Chem. Chem. Phys. 10 (2008) 2646.
[20] N. Yamazaki, I. Washio, Y. Shibasaki, M. Ueda, Org. Lett. 8 (2006) 2321.
[21] Y.-Z. Li, Z.-M. Li, F. Li, Q.-R. Wang, F.-G. Tao, Org. Biomol. Chem. 3 (2005) 2513.
[22] N.L. Allinger, J. Am. Chem. Soc. 99 (1977) 8127.
[23] G. Chang, W.C. Guida, W.C. Still, J. Am. Chem. Soc. 111 (1989) 4379.
[24] HyperChem(TM) Professional 8.0, Hypercube, Inc., 1115 NW 4th Street, Gainesville, Florida 32601, USA.
[25] Y. Zhao, D.G. Truhlar, Theor. Chem. Acc. 120 (2008) 215.
[26] M.J. Frisch, G.W. Trucks, H.B. Schlegel, G.E. Scuseria, M.A. Robb, J.R. Cheeseman, G. Scalmani, V. Barone, B. Mennucci, G.A. Petersson, H. Nakatsuji, M. Caricato, X. Li, H.P. Hratchian, A.F. Izm Aylov, J. Bloino, G. Zheng, J.L. Sonnenberg, M. Hada, M. Ehara, K. Toyota, R. Fukuda, J. Hasegawa, M. Ishida, T. Nakajima, Y. Honda, O. Kitao, H. Nakai, T. Vreven, J.A. Montgomery, J.E. Peralta, F. Ogliaro, M. Bearpark, J.J. Heyd, E. Brothers, K.N. Kudin, V.N. Staroverov, R. Kobayashi, J. Normand, K. Raghavachari, A. Rendell, J.C. Burant, S.S. Iyengar, J. Tomasi, M. Cossi, N. Rega, J.M. Millam, M. Klene, J.E. Knox, J.B. Cross, V. Bakken, C. Adamo, J. Jaramillo, R. Gomperts, R.E. Stratmann, O. Yazyev, A.J. Austin, R. Cammi, C. Pomelli, J.W. Ochterski, R.L. Martin, K. Morokuma, V.G. Zakrzewski, P. Voth, G.A. Salvador, J.J. Dannenberg, S. Dapprich, A.D. Daniels, O. Farkas, J.B. Foresman, J.V. Ortiz, J. Cioslowski, D.J. Fox, Gaussian 09, Revision, A.02, Gaussian, Inc., Wallingford, CT, 2009.
[27] (a) R. Podeszwa, R. Bukowski, K. Szalewicz, J. Phys. Chem. A 110 (2006) 10345;
(b) J.G. Hill, J.A. Platts, H.-J. Werner, Phys. Chem. Chem. Phys. 8 (2006) 4072.
[28] J. Shoolery, A Basic Guide to NMR, vol. II, 3rd ed., Stan's Library, 2008, http://dx.doi.org/10.3247/sl2nmr08.012.
[29] (a) U. Haeusermann, M. Dolg, H. Stoll, H. Preuss, Mol. Phys. 78 (1993) 1211;
(b) W. Kuechle, M. Dolg, H. Stoll, H. Preuss, J. Chem. Phys. 100 (1994) 7535;
(c) T. Leininger, A. Nicklass, H. Stoll, M. Dolg, P. Schwerdtfeger, J. Chem. Phys. 105 (1996) 1052.
[30] J.D. Dunitz, R. Taylor, Chem. Eur. J. 3 (1997) 89.
[31] (a) M. Quiros, F. Rebolledo, R. Liz, V. Gotor, Tetrahedron: Asymmetry 8 (1997) 3035;
(b) H.-L. Huang, L.T. Liu, F.-S. Chen, H. Ku, Tetrahedron: Asymmetry 9 (1998) 1637;
(c) D. Liu, W.-Z. Gao, C.-J. Wang, X.-M. Zhang, Angew. Chem. Int. Ed. 44 (2005) 1687.
[32] The residual ruthenium (in 10 ml 10% liquor of HNO_3) was determined by ICP (P-4010). No leaching of Ru could be found until the limit of detection (0.02 ppm).